Ab initio calculations of second-, third-, and fourth-order elastic constants for single crystals

Hao Wang[1,2] and Mo Li[1,*]
[1]*School of Materials Science and Engineering, Georgia Institute of Technology, Atlanta, Georgia 30332, USA*
[2]*School of Physics, Georgia Institute of Technology, Atlanta, Georgia 30332, USA*
(Received 30 October 2008; revised manuscript received 12 March 2009; published 3 June 2009)

We present a general scheme to calculate the second-, third-, and fourth-order elastic constants of single crystals with arbitrary symmetry by employing *ab initio* density-functional theory. The method utilizes a series of homogeneous deformation strains applied to a crystalline system to obtain the internal energy-strain relations. From the nonlinear least-squares fitting, we obtain the elastic constants from the coefficients of the fitted polynomials of the internal energy functions. We applied this method first to four fcc metal crystals, Cu, Al, Au, and Ag. The calculated second-, third-, and fourth-order elastic constants are compared with the available experimental data and other theoretical calculations and found very good agreement. Since accurate determination of higher-order elastic constants, in particular, the fourth-order elastic constants from experiment, is still a challenge, the theoretical approach presented here is certainly of a great help to fill the gap.

DOI: 10.1103/PhysRevB.79.224102 PACS number(s): 62.20.D−, 71.15.Mb, 71.55.Ak

I. INTRODUCTION

In the theory of linear elasticity, infinitesimal deformation strains are assumed. As a result, the second-order elastic constants (SOECs) are sufficient to describe the elastic stress-strain response and wave propagation in solids.[1,2] In case of finite strains, the theory of nonlinear elasticity is required.[3–7] It is well known that third-order elastic constants (TOECs) are important quantities to describe nonlinear mechanical effects. In many occasions, even higher-order elastic constants such as the fourth-order ones may be needed to describe the nonlinear effect. As shown by Ghate,[8] for a crystal with cubic symmetry subject to a simple shear with a finite shear strain, e.g., η_{12}, the elastic energy expanded in Taylor series to the third order in terms of the strain parameter gives $E=E_0+\psi_2+\psi_3$, where E_0 is the energy of the undeformed sample, $\psi_2=C_{44}\eta_{12}^2/2$, and $\psi_3=0$. The last result shows that nonlinear effect, if there is any, would not be present in this case. To reach higher-order accuracy, one would expect to add the fourth-order term, $\psi_4=\frac{2}{3}C_{4444}\eta_{12}^4$, in which the C_{4444} is the fourth-order elastic constant (FOEC). In many real applications beyond this simple example, there are plenty of cases where the high-order elastic constants are needed that are not merely limited in the area of mechanics. For example, TOECs, FOECs, and higher-order elastic constants have been used to interpret anharmonic phenomena in solid-state physics, such as phonon-phonon interaction, Grűneisen parameters,[9] etc. They also have appeared in the development of ion-electron pseudopotentials[10] or empirical interatomic potentials.[11] Recently, the nonlinear effects in elastic[12–14] and piezoelectric properties[15,16] have drawn many interests in nanoscale materials where nonlinear effects become significant. Of particular interest are those activities that involve the fourth-order elastic constants in the description of nonlinear phenomena such as intermodulation in thickness-shear and trapped-energy resonators,[17,18] the generation of third harmonics in finite-amplitude waves,[19] the description of shock-compression stress-strain curves,[20,21] and in the nonlinear constitutive equations for thermoelectroelastic materials.[22]

Many experiments have been performed to determine SOECs and high-order elastic constants.[23] However, for crystals with low symmetry or with low-yield stress, to obtain a complete set of TOECs is still not a simple task. For FOECs the difficult becomes more acute. As a result, there are few experimental values for the FOECs available so far. A feasible alternative is theoretical calculations. In the past two decades, several theoretical methods have been developed to calculate higher-order elastic constants for single crystals. For the TOECs, there are quite a few methods available, including empirical interatomic force-constant model,[24,25] molecular-dynamics simulation using fluctuation formula,[26,27] the methods of homogeneous deformation based on empirical or the first-principles total-energy methods,[28] and other quantum calculations.[29–31] The approaches used in the TOEC calculations, in principle, could be extended in the calculations of the FOECs, but certain care must be exercised due to the increasing complexity of the formulations and the demand for high accuracies needed in the computation.

In this work, we shall employ the method similar to that practiced earlier by Nielsen and Martin.[29,30] In this approach, the homogeneous deformation strain is applied to the system and usually simple deformation modes are used such as uniaxial tension or compression, simple or pure shear, and other combinations of homogeneous strains. The total elastic energies of the system subject to these deformations are calculated using *ab initio* methods employing the density-functional theory (DFT). The internal energy-strain curves under the various strains, which are often far beyond those of the linear elastic limit, are numerically fitted using polynomials. Because of the deliberate selection of the homogeneous deformation modes, the coefficients in the internal energy polynomial functions are simple combinations of the second-, third-, or fourth-order elastic constants. Through the numerical fitting, we can obtain the elastic constants straightforwardly. Recently, the same method was used in the first-principles quantum mechanics calculations of the third-order elastic constants by Zhao *et al.*[32] and Lopuszynski and Majewski[33] in single crystals with covalent bond. Their results show good agreement with experiments. In this paper, we extend this method to calculating the fourth-order elastic constants, which to the best of our knowledge has not been systematically performed and tested.

This paper is organized as follows. In Sec. II, we give a general introduction of nonlinear elasticity with a particular attention paid to the relation of the higher-order elastic constants with the internal energy. In Sec. III, we present the methods of applying homogeneous deformation to the system and *ab initio* calculation to obtain the internal energy-deformation strain relations. In Sec. IV, we give the results for the calculated fourth-order elastic constants for the four fcc metals, Cu, Al, Au, and Ag, along with the second- and third-order ones. Available results from experiments and other theoretical methods are also shown for comparison. In Sec. V, we draw conclusions from this work.

II. THEORY OF NONLINEAR ELASTICITY

For a solid-body subject to a finite deformation, the configuration of a material point in the system after deformation is represented as $x=x(a)$, where a is the initial configuration at the equilibrium state. The deformation gradient is defined by

$$J_{ij} = \frac{\partial x_i}{\partial a_j}, \tag{1}$$

where i and $j(=1,2,3)$ represent the Cartesian coordinates. Then the Lagrangian strain tensor is defined as

$$\eta = \frac{1}{2}(J^T J - I), \tag{2}$$

where I is the unit matrix.

The internal energy and the free energy are related to the Lagrangian strain tensor in the theory of nonlinear elasticity through Taylor-series expansion in terms of the strain tensor,[2–4]

$$\begin{aligned} U(a,\eta_{ij},S) = U(a,S) &+ (1/2!)V\sum_{ijkl} C^S_{ijkl}\eta_{ij}\eta_{kl} \\ &+ (1/3!)V\sum_{ijklmn} C^s_{ijklmn}\eta_{ij}\eta_{kl}\eta_{mn} \\ &+ (1/4!)V\sum_{ijklmnpq} C^s_{ijklmnpq}\eta_{ij}\eta_{kl}\eta_{mn}\eta_{pq} + \cdots, \end{aligned} \tag{3}$$

$$\begin{aligned} F(a,\eta_{ij},T) = F(a,T) &+ (1/2!)V\sum_{ijkl} C^T_{ijkl}\eta_{ij}\eta_{kl} \\ &+ (1/3!)V\sum_{ijklmn} C^T_{ijklmn}\eta_{ij}\eta_{kl}\eta_{mn} \\ &+ (1/4!)V\sum_{ijklmnpq} C^T_{ijklmnpq}\eta_{ij}\eta_{kl}\eta_{mn}\eta_{pq} + \cdots, \end{aligned} \tag{4}$$

where $U(a,\eta_{ij},S)$ is the internal energy, $F(a,\eta_{ij},S)$ is the Helmholtz free energy, T is the temperature, S is the entropy, and V is the volume of the system.

The elastic constants of second, third, fourth, and higher orders are defined as the second-, third-, fourth-, and higher-order derivatives of the above functions with respect to the strain, respectively. The adiabatic elastic constants of second, third, and fourth orders are

$$C^S_{ijkl} = V^{-1}(\partial^2 U/\partial\eta_{ij}\,\partial\,\eta_{kl})_{S\eta}, \tag{5}$$

$$C^S_{ijklmn} = V^{-1}(\partial^2 U/\partial\eta_{ij}\,\partial\,\eta_{kl}\,\partial\,\eta_{mn})_{S\eta}, \tag{6}$$

$$C^S_{ijklmnpq} = V^{-1}(\partial^2 U/\partial\eta_{ij}\,\partial\,\eta_{kl}\,\partial\,\eta_{mn}\,\partial\,\eta_{pq})_{S\eta}. \tag{7}$$

And the isothermal elastic constants are

$$C^T_{ijkl} = V^{-1}(\partial^2 F/\partial\eta_{ij}\,\partial\,\eta_{kl})_{T\eta}, \tag{8}$$

$$C^T_{ijklmn} = V^{-1}(\partial^2 F/\partial\eta_{ij}\,\partial\,\eta_{kl}\,\partial\,\eta_{mn})_{T\eta}, \tag{9}$$

$$C^T_{ijklmnpq} = V^{-1}(\partial^2 F/\partial\eta_{ij}\,\partial\,\eta_{kl}\,\partial\,\eta_{mn}\,\partial\,\eta_{pq})_{T\eta}. \tag{10}$$

These elastic constants are defined at the initial configuration a, where η_{ij} are measured from a. The initial state as represented by a is in fact arbitrary but must be in equilibrium. In this work, we have the initial state a at $\eta=0$, a undeformed state. Since our *ab initio* calculations are performed at 0 K, $F=U-TS=U$, so $C^S=C^T$. We will not distinguish those two types of elastic constants in the following.

We can simplify the notations in the tensors by using the Voigt notation ($11\rightarrow1$, $22\rightarrow2$, $33\rightarrow3$, $23\rightarrow4$, $31\rightarrow5$, and $12\rightarrow6$). We have therefore for the strain tensors $\eta_{11}\rightarrow\eta_1$, $\eta_{22}\rightarrow\eta_2$, $\eta_{33}\rightarrow\eta_3$, $\eta_{23}\rightarrow\eta_4/2$, $\eta_{31}\rightarrow\eta_5/2$, and $\eta_{12}\rightarrow\eta_6/2$. Equations (3) and (4) now can be written as

$$\begin{aligned} V^{-1}&[U(a,\eta) - U(a,0)] \\ &= \frac{1}{2!}\sum_{i,j=1,6} c_{ij}\eta_i\eta_j + \frac{1}{3!}\sum_{i,j,k=1,6} c_{ijk}\eta_i\eta_j\eta_k \\ &\quad + \frac{1}{4!}\sum_{i,j,k,l=1,6} c_{ijkl}\eta_i\eta_j\eta_k\eta_l + \cdots. \end{aligned} \tag{11}$$

For single crystals with cubic symmetry, we can express Eq. (11) in the second-, third- and fourth-order terms of the strain tensor,

$$V^{-1}[U(a,\eta) - U(a,0)] = \psi_2 + \psi_3 + \psi_4\cdots, \tag{12}$$

where

$$\begin{aligned} \psi_2 = &\frac{1}{2}c_{11}(\eta_1^2+\eta_2^2+\eta_3^2) + c_{12}(\eta_1\eta_2+\eta_2\eta_3+\eta_3\eta_1) \\ &+ \frac{1}{2}c_{44}(\eta_4^2+\eta_5^2+\eta_6^2), \end{aligned} \tag{13}$$

$$\begin{aligned} \psi_3 = &\frac{1}{6}c_{111}(\eta_1^3+\eta_2^3+\eta_3^3) \\ &+ \frac{1}{2}c_{112}(\eta_2\eta_1^2+\eta_3\eta_1^2+\eta_1\eta_2^2+\eta_1\eta_3^2+\eta_2\eta_3^2+\eta_3\eta_2^3) \\ &+ c_{123}\eta_1\eta_2\eta_3 + \frac{1}{2}c_{144}(\eta_1\eta_4^2+\eta_2\eta_5^2+\eta_3\eta_6^2) \\ &+ \frac{1}{2}c_{155}(\eta_2\eta_4^2+\eta_3\eta_4^2+\eta_1\eta_5^2+\eta_3\eta_5^2+\eta_1\eta_6^2+\eta_2\eta_6^2) \\ &+ c_{456}\eta_4\eta_5\eta_6, \end{aligned} \tag{14}$$

and[8]

$$\psi_4 = \frac{1}{24}C_{1111}(\eta_1^4+\eta_2^4+\eta_3^4)+\frac{1}{6}C_{1112}[\eta_1^3(\eta_2+\eta_3)+\eta_2^3(\eta_3+\eta_1)+\eta_3^3(\eta_1+\eta_2)]+\frac{1}{4}C_{1122}(\eta_1^2\eta_2^2+\eta_2^2\eta_3^2+\eta_3^2\eta_1^2)$$
$$+\frac{1}{2}C_{1123}(\eta_1^2\eta_2\eta_3+\eta_2^2\eta_3\eta_1+\eta_3^2\eta_1\eta_2)+\frac{1}{4}C_{1144}(\eta_1^2\eta_4^2+\eta_2^2\eta_5^2+\eta_3^2\eta_6^2)+\frac{1}{4}C_{1155}[\eta_1^2(\eta_5^2+\eta_6^2)+\eta_2^2(\eta_4^2+\eta_6^2)+\eta_3^2(\eta_4^2+\eta_5^2)]$$
$$+\frac{1}{2}C_{1255}[\eta_1\eta_2(\eta_4^2+\eta_5^2)+\eta_2\eta_3(\eta_5^2+\eta_6^2)+\eta_1\eta_3(\eta_4^2+\eta_6^2)]+\frac{1}{2}C_{1266}(\eta_1\eta_2\eta_6^2+\eta_2\eta_3\eta_4^2+\eta_1\eta_3\eta_5^2)$$
$$+C_{1456}[\eta_4\eta_5\eta_6(\eta_1+\eta_2+\eta_3)]+\frac{1}{24}C_{4444}(\eta_4^4+\eta_5^4+\eta_6^4)+\frac{1}{4}C_{4455}(\eta_4^2\eta_5^2+\eta_5^2\eta_6^2+\eta_6^2\eta_4^2). \quad (15)$$

As shown above, there are three independent SOECs (c_{11}, c_{12}, and c_{44}), six TOECs (c_{111}, c_{112}, c_{123}, c_{144}, c_{155}, and c_{456}), and 11 FOECs (c_{1111}, c_{1112}, c_{1122}, c_{1123}, c_{1144}, c_{1155}, c_{1255}, c_{1266}, c_{1456}, c_{4444}, and c_{4455}). As shown below, these elastic constants can be obtained in the theoretical calculations by subjecting the system to various simple deformation strains, provided also that the system does not have any polymorphic phase transition and internal deformation under these strains.

The Lagrangian stress is defined as the first-order derivative of the internal energy or Helmholtz free energy with respect to the strain tensor,

$$\sigma_{ij} = V^{-1}(\partial U/\partial \eta_{ij}) = V^{-1}(\partial F/\partial \eta_{ij}), \quad (16)$$

which can also be used also to evaluate the elastic constants.[29,30]

III. METHODS OF HOMOGENEOUS DEFORMATION AND *AB INITIO* COMPUTATION

Equations (11) and (13)–(15) suggest that we can treat the internal energy difference as a polynomial function of the strain η_{ij}. Since there are six strain components in the strain tensor when the system is rotation-free, one must select specific deformation modes to reduce the number of the strain components that will appear in the internal energy function. To make this feasible, we can select certain simple deformation or loading modes such that the strain tensor η_{ij} only has one or a few components. As a result, the coefficients in the polynomial are simple combinations of the elastic constants. For example, if we choose to subject the system with a uniaxial tension along the x direction (or $i, j=1$), the tensile strain, $\eta_1=\xi$ and the rest of the strain components are all zero, that is, $\eta=(\xi,0,0,0,0,0,0)$. From Eqs. (13)–(15), we can see that this selection of the deformation mode results in an internal energy that can be expressed as a polynomial of the strain parameter ξ, that is, $V^{-1}[U(0,\xi)-U(0,0)]=1/2c_{11}\xi^2+1/6c_{111}\xi^3+1/24c_{1111}\xi^4$. To simplify the matter further, we can use only one scalar parameter ξ for all nonzero strain components. The selection of the different deformation modes leads to different strains used in this work, which are labeled as η_α, $\alpha=A,B,\ldots,K$, and listed in Table I. There are total of 11 independent deformation modes we use in this work. Therefore, each time we apply a certain type of deformation mode to the crystal system, we use a specific strain parameter η_α in which there is only one strain parameter ξ that we can vary. That is, when we substitute a particular type of strain to Eqs. (11)–(16), we will have the polynomial function for the internal energy function and the stress,

TABLE I. For each type of strain modes, $\eta_\alpha(\xi)$, $\alpha=A,B,\ldots,K$, the internal energy is expressed as a polynomial function of ξ. The coefficients P_2,P_3,P_4 in Eq. (17) are shown as the linear combinations of the second-, third-, and fourth-order elastic constants, respectively.

Strain type	P_2	P_3	P_4
$\eta_A=(\xi,0,0,0,0,0)$	$\frac{1}{2}C_{11}$	$\frac{1}{6}C_{111}$	$\frac{1}{24}C_{1111}$
$\eta_B=(\xi,\xi,0,0,0,0)$	$C_{11}+C_{12}$	$\frac{1}{3}C_{111}+C_{112}$	$\frac{1}{12}C_{1111}+\frac{1}{3}C_{1112}+\frac{1}{4}C_{1122}$
$\eta_C=(\xi,-\xi,0,0,0,0)$	$C_{11}-C_{12}$	0	$\frac{1}{12}C_{1111}-\frac{1}{3}C_{1112}+\frac{1}{4}C_{1122}$
$\eta_D=(\xi,0,0,2\xi,0,0)$	$\frac{1}{2}C_{11}+2C_{44}$	$\frac{1}{6}C_{111}+2C_{144}$	$\frac{1}{24}C_{1111}+C_{1144}+\frac{2}{3}C_{4444}$
$\eta_E=(\xi,0,0,0,0,2\xi)$	$\frac{1}{2}C_{11}+2C_{44}$	$\frac{1}{6}C_{111}+2C_{155}$	$\frac{1}{24}C_{1111}+C_{1155}+\frac{2}{3}C_{4444}$
$\eta_F=(0,0,0,2\xi,2\xi,2\xi)$	$6C_{44}$	$8C_{456}$	$2C_{4444}+12C_{4455}$
$\eta_G=(0,0,0,2\xi,0,0)$	$2C_{44}$	0	$\frac{2}{3}C_{4444}$
$\eta_H=(\xi,\xi,0,0,0,2\xi)$	$C_{11}+C_{12}+2C_{44}$	$\frac{1}{3}C_{111}+C_{112}+4C_{155}$	$\frac{1}{12}C_{1111}+\frac{1}{3}C_{1112}+\frac{1}{4}C_{1122}+2C_{1155}+2C_{1266}+\frac{2}{3}C_{4444}$
$\eta_I=(\xi,\xi,0,2\xi,0,0)$	$C_{11}+C_{12}+2C_{44}$	$\frac{1}{3}C_{111}+C_{112}+2C_{144}+2C_{155}$	$\frac{1}{12}C_{1111}+\frac{1}{3}C_{1112}+\frac{1}{4}C_{1122}+C_{1144}+C_{1155}+2C_{1255}+\frac{2}{3}C_{4444}$
$\eta_J=(\xi,0,0,2\xi,2\xi,2\xi)$	$\frac{1}{2}C_{11}+3C_{44}$	$\frac{1}{6}C_{111}+2C_{144}+4C_{155}+8C_{456}$	$\frac{1}{24}C_{1111}+C_{1144}+2C_{1155}+8C_{1456}+2C_{4444}+12C_{4455}$
$\eta_K=(\xi,\xi,\xi,0,0,0)$	$\frac{3}{2}C_{11}+3C_{12}$	$\frac{1}{2}C_{111}+3C_{112}+C_{123}$	$\frac{1}{8}C_{1111}+C_{1112}+\frac{3}{4}C_{1122}+\frac{3}{2}C_{1123}$

$$V^{-1}[U(a,\xi) - U(a,0)] = f_\alpha[\eta_\alpha(\xi)] = P_2\xi^2 + P_3\xi^3 + P_4\xi^4 + O(\xi^5), \tag{17}$$

$$V^{-1}(\partial U/\partial \eta_i) = \sigma_\alpha[\eta_\alpha(\xi)] = Q_1\xi + Q_2\xi^2 + Q_3\xi^3 + O(\xi^4), \tag{18}$$

where $\alpha=A,B,\ldots,K$ and the coefficients, P_2, P_3, P_4, Q_1, Q_2, and Q_3, are related to the elastic constants. As mentioned earlier, we have 11 of those functions for the internal energies and stresses corresponding to the different strains that are needed to fit 11 of the FOECs (see Table I).

To implement the different deformation modes in our calculation, we need to have the deformation gradient matrix J. As mentioned at Eq. (2), J is related to the strain η. Inversion of Eq. (2) gives

$$J_{ij} = \delta_{ij} + \eta_{ij} - \frac{1}{2}\sum_k \eta_{ki}\eta_{kj} + \cdots. \tag{19}$$

For a given strain η, in general, J is not unique but this is not a problem since the Lagrange strain brings rotational invariance of total energy. Furthermore, for the system without rotation Eq. (19) provides a unique relation. We then apply the deformation gradient J to each of the crystal lattice vector r_i, where i is the lattice index. The deformed or strained crystal is obtained then from $R_i=J_{ij}r_j$.

For each specific deformation mode in our calculation labeled as $\alpha=A,B,\ldots,K$, we change the value of ξ from $-|\xi_{\max}|$ to $+|\xi_{\max}|$ with a finite step size $\Delta\xi$, where $\xi_{\max}$ is the maximum value for the strain parameter chosen for each deformation calculation. As we show below, the values for both $\xi_{\max}$ and $\Delta\xi$ are important to obtaining high-quality data, which are needed for the calculations of the higher-order elastic constants. For each value of ξ, the total energy and stress tensor of the deformed crystal are calculated by *ab initio* method. Therefore, in our case, the 11 internal energy polynomial curves are calculated separately.

To obtain the coefficients in Eqs. (17) and (18) we fit the polynomial curves, $f(\xi)$ and $\sigma(\xi)$. Using nonlinear least-squares fitting, we first obtain the values for the coefficients P_2,P_3,P_4 and Q_1,Q_2,Q_3. Each of these coefficients is a linear combination of the second-, third-, or fourth-order elastic constants. The detailed relations for P_i and the elastic constants are given in Table I. Then from these relations, we can obtain the elastic constants.

In this paper, we will use fcc single crystal as examples because first, they do not possess internal deformation related to the absence of inversion symmetry. Second, as compared with other types of crystals, the fcc metals have the complete set of the second- and third-order elastic constants available from experiments, so we have those reference data to compare. Third, since the fourth-order elastic constants are very difficult to obtain in experiment and only available in theoretical calculations, our calculation would be more valuable in providing the data needed for these systems. Since we propose to use DFT to compute the FOECs, our goal is more on testing the feasibility than on general utility of this technique which may be extended later to other systems with more industrial and commercial relevance, which includes some covalent crystals that have the FOECs available from experiments.[23]

As mentioned before, for the cubic crystals, there are 11 independent fourth-order elastic constants, so we need at least 11 types of homogeneous deformation strain parameters since for each deformation mode, we can only identify one coefficient as a linear combination of a certain number of the fourth-order elastic constants. We should mention that from the stress-strain relation [Eq. (16)] we could in principle obtain the fourth-order elastic constants as originally shown by Nielsen and Martin.[29,30] In this work, however, we shall focus on the method based on the internal energy-strain relation [Eqs. (11)–(15)].

To obtain the internal energy or strain energy at $T=0$ and with only external force exerted by applying strain, we performed the *ab initio* calculations using the Vienna *ab initio* simulation package (VASP) developed by the Hafner Research Group at the University of Vienna.[34] VASP uses pseudopotentials or the projector-augmented wave method and a plane-wave basis set. To obtain lattice parameters that are in better agreement with experimental values, we used the exchange-correlation energy evaluated by local-density approximation (LDA) for Cu and Al; for Ag and Au we used generalized gradient approximation (GGA). Ultrasoft pseudopotentials were always employed to describe the electron-ion interactions.[35] Since high accuracy is needed to evaluate the FOECs, to test the convergence of the total energy and the FOECs, we used the k-point mesh up to $30\times30\times30$ in our calculations following the Monkhost-Pack scheme. As our experience shows, for up to $24\times24\times24$ mesh size it is sufficient to reach the desired convergence for the total energy as well as for the fourth-order elastic constants. We took the cutoff energy set at $E_{cutoff}^{\mathrm{Ag}}=500$ eV, $E_{cutoff}^{\mathrm{Cu}}=490$ eV, $E_{cutoff}^{\mathrm{Al}}=500$ eV, and $E_{cutoff}^{\mathrm{Au}}=450$ eV, which as our convergence test shows are sufficiently large for the total energy to converge to the equilibrium state and particularly for the fourth-order elastic constants to converge well.

Take Cu as an example. Figure 1(a) shows the internal energy convergence with the k-point grid size. Starting from $14\times14\times14$ k-point grid, the internal energy is well converged after $24\times24\times24$ mesh size. Figure 1(b) is a zoom-in picture of Fig. 1(a), it shows at the k-point grid size we used up to $30\times30\times30$, the internal energy convergence at meV level. Figure 2 shows how the selection of the cutoff energy affects the internal energy convergence. As shown, $E_{cutoff}^{\mathrm{Cu}}=490$ eV is sufficient. The calculated lattice constant of the fcc Cu at the equilibrium state is shown in Fig. 3; so we use 3.64 Å as the equilibrium lattice parameter to construct our supercell in the simulation work later on.

The convergence test for the calculated elastic constants of Cu is presented in Figs. 4 and 5. The results show a stronger dependence of the fourth-order elastic constants $C_{1111},C_{1112},C_{4444},C_{1155}$ on the cutoff energy and Monkhost-Pack k-point mesh size as compared with the total energy. From the four samples, it is clear that the FOECs converge rapidly after the k-point mesh size reaches $24\times24\times24$. For the selected parameters ($E_{cutoff}^{\mathrm{Cu}}=490$ eV and $30\times30\times30$

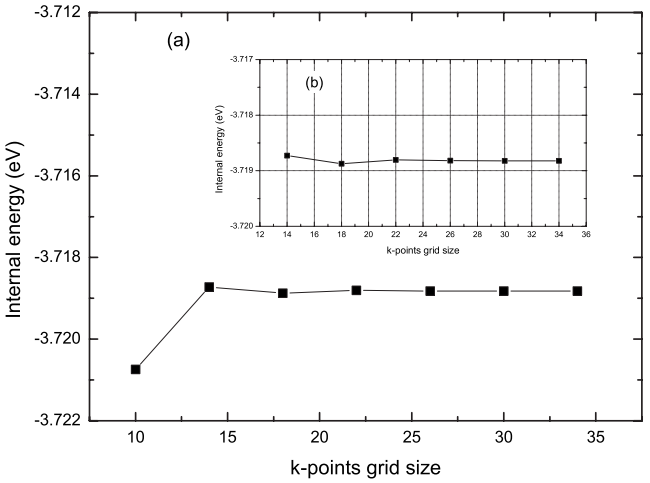

FIG. 1. (a) The dependence of the first-principles results of the internal energy of Cu on the *k*-point mesh size. The energy converges well when the *k*-point mesh size goes beyond $14\times14\times14$. (b) The inset is the zoom-in picture of the internal energy variation with the *k*-point mesh size. It shows that the energy converges to meV level at the choice of the *k*-point mesh size.

k-point mesh size), the relative difference between the FOECs obtained with this mesh size and with the smaller mesh size of $28\times28\times28$ is less than 1%. This difference is less than the standard error when we perform polynomial fitting. Therefore, we adopt the following criterion in our selection of the *k*-point mesh size: in the converging region (the mesh size is larger than $24\times24\times24$), if the difference of the FOECs calculated with two successive *k*-point mesh sizes are within 1%, we shall pick the later as our choice. The same principle applies to cutoff energy selection. This approach allows us to save considerable amount of computing time.

The lattice constants we obtained for Cu, Au, Al, and Ag are very close to the experimental measurements. The results are listed in Table II. Ag has a relatively larger deviation as

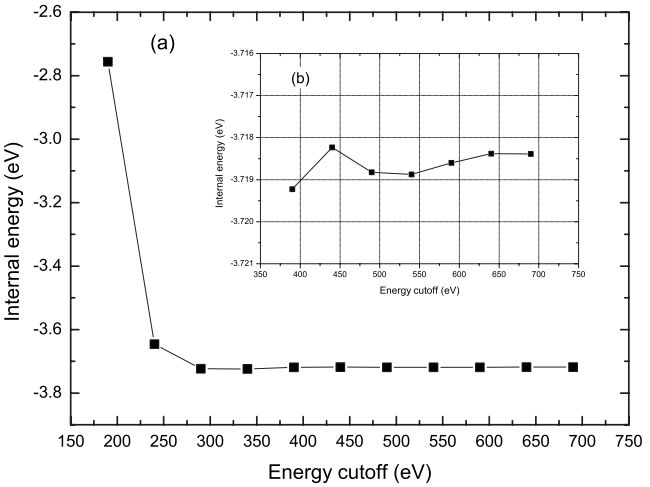

FIG. 2. (a) The calculated internal energy of Cu as a function of the cutoff energy. (b) The inset is the zoom-in picture of the energy that converges within meV level when the cutoff energy is beyond 340 eV. In our calculation, we chose E_{cutoff}^{Cu}=490 eV.

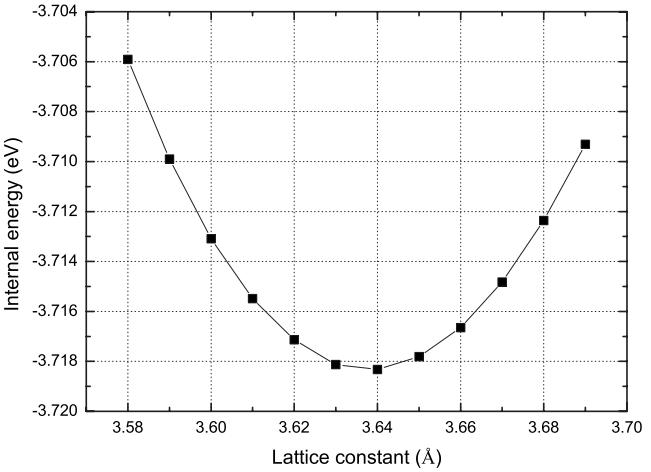

FIG. 3. In the calculated internal energy of Cu as a function of lattice constant, the equilibrium lattice parameter is found to be 3.64 Å, which is determined from the corresponding minimum value of the internal energy.

compared with other metals in this group. As seen below, this larger error for Ag in the lattice constant may also be the reason that the elastic constants calculated show larger dif-

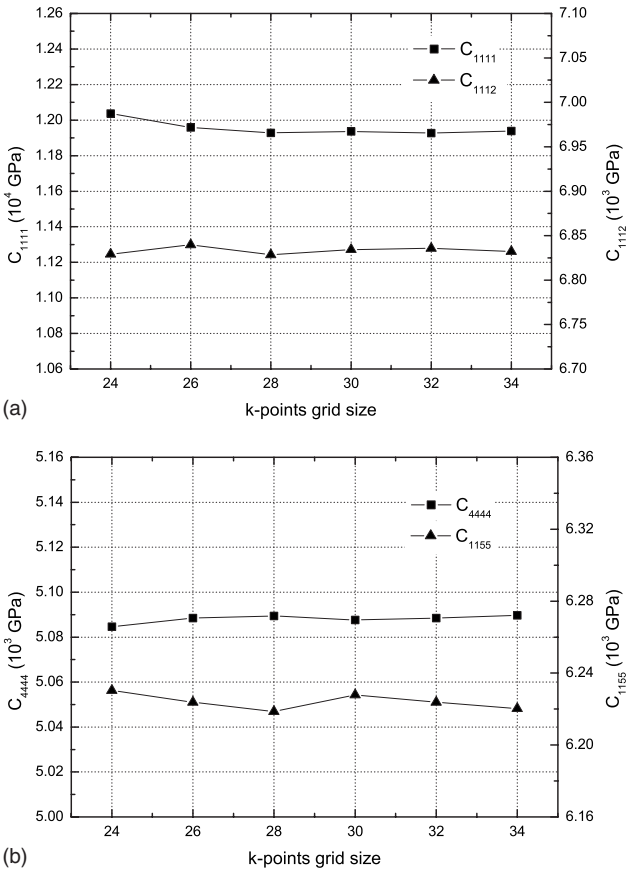

FIG. 4. The dependence of four fourth-order elastic constants $C_{1111}, C_{1112}, C_{4444}, C_{1155}$ on the Monkhost-Pack *k*-point mesh size. With E_{cutoff}^{Cu}=490 eV applied to all mesh sizes, the relative difference between two successive values of examined constants in our test after $24\times24\times24$ is lower than 1%.

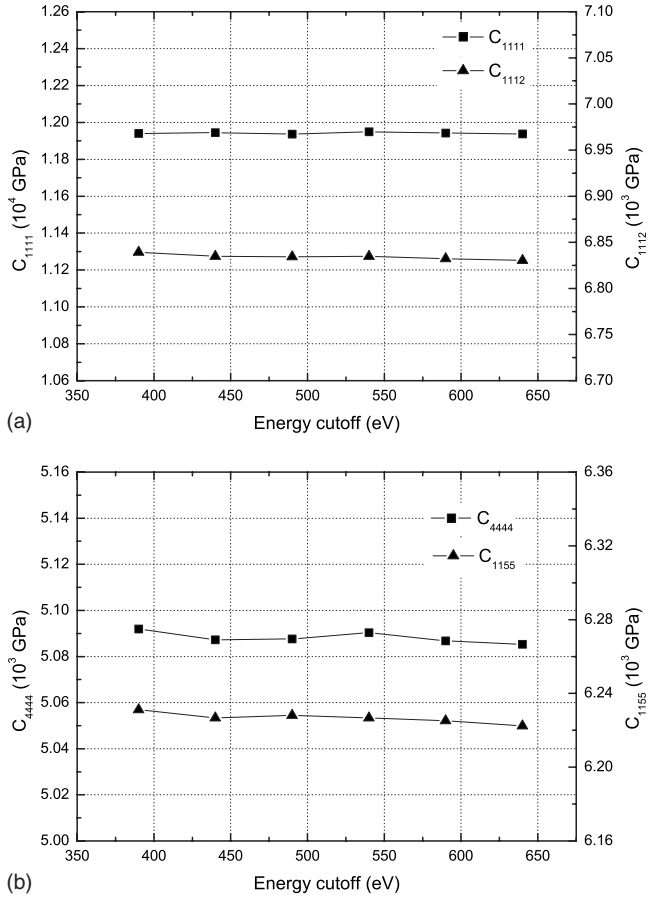

FIG. 5. The dependence of the four fourth-order elastic constants $C_{1111}, C_{1112}, C_{4444}, C_{1155}$ on the cutoff energy. With $30\times30\times30$ k-point mesh size applied to all points, the relative difference between two successive values of examined constants in our test is lower than 1%.

ferences as compared with the reference data. In addition, we would like to mention that since our calculation is performed at 0 K and the experimental values are measured at room temperature, certain differences in the lattice constants and elastic constants should be anticipated. Based on those calculated lattice constants, we prepared supercells to calculate energy-strain curves. The deformation is implemented for each supercell using the deformation gradient from Eq. (19) in the incremental fashion governed by the two parameters $\xi_{\max}$ and $\Delta\xi$.

TABLE II. The calculated and experimentally determined lattice constants for Cu, Al, Au, and Ag. The unit is Å.

	This work	Expt.
Cu	3.64	3.62[a]
Al	4.04	4.05[b]
Au	4.07	4.08[a]
Ag	4.02	4.09[a]

[a]Reference 36 (T=25 °C).
[b]Reference 36 (T=24.8 °C).

IV. RESULTS

Table III shows all elastic constants up to the fourth-order ones calculated using the above methods. By inspecting the data in (a) of Table III, it becomes obvious that the values of the SOECs [c_{11}, c_{12}, and c_{44} in (a) of Table III] are the best in agreement with the experimental ones. The differences are well within 5% for Cu, Au, and Al but a large deviation around 20% is found for all three SOECs for Ag, which may share the same origin as that in the lattice constant calculated. Nevertheless, the excellent overall agreement of the SOECs provides the support for the approaches used in this work, which appears more feasible as compared with other *ab initio* calculations.[41]

As compared with the SOECs, the TOECs are much difficult to measure experimentally. As a result, only a small number of fcc metals have a full set of TOECs available that include Cu, Au, Al, and Ag.[23,37–39] By inspecting the data in (b) of Table III, we see that the overall agreement between our calculated TOECs for all fcc metals listed and the existing experimental values is very good. For Cu and Al, we tabulated three sets of experimental data, one at 4.2 K for Cu, one at 80 K for Al, and two at RT for both metals. We see that our *ab initio* calculation captures both the signs and the magnitude of the TOECs very well. A small positive C_{456} for Cu and C_{123} for Al are reproduced well, and both C_{111} and C_{112} agree with experimental values very well, especially for Al. For Au, the opposite sign was found for C_{456}, which we suspect is caused by the temperature effect, as seen for Cu, since the experimental value is at RT while our calculation is at 0 K. A set of TOECs for Cu from a total-energy calculation by Soma and Hiki is listed also in Table III for comparison.

The discrepancies found in the TOECs could be originated from many sources in experiments as well as in our calculations. For experimental measurement, as noted by Hiki and Granato,[23,42] dislocations could be easily generated when the samples are under external loading during measurement since pure single crystals have relatively low-yield stress. The dislocations would cause interference in the ultrasound waves leading to errors. For this reason, those higher-order elastic constants (C_{144}, C_{155}, C_{456}, etc.) that involve shear strain have much larger uncertainties. On the other hand, in *ab initio* calculation, as noted in the work of Zhao *et al.*,[32] the strain range $\xi_{\max}$ is an important parameter affecting the accuracy of the elastic constants. This is understandable as the nonlinear elastic constants become significant when the strains are larger. Another parameter is the strain incremental value, $\Delta\xi$. Too large a value could lead to systematic errors.

For the above reasons, the FOECs are much difficult to obtain in our calculations. To get converging values for them, besides the large k-point mesh size and energy cutoffs, we need a larger strain range $\xi_{\max}$. As for Cu, for example, C_{1111} converges only after $\xi_{\max}\sim0.15$ (see Fig. 6). The reason comes from that at small strain range, ψ_4 is much less than ψ_2 and ψ_3 as well. Thus, if the magnitude of $\xi_{\max}$ is not sufficiently large, large fitting errors will appear, resulting mainly from the fitted coefficient of ψ_4. This situation will be improved when those errors are not comparable with the

TABLE III. The calculated (a) second-, (b) third-, and (c) fourth-order elastic constants of Cu, Ag, Au, and Al. Experimental results and other theoretical calculations are also shown. The unit is in GPa.

(a)

	C_{11}	C_{12}	C_{44}
Cu	167.8[a]	113.5[a]	74.5[a]
	169[b]	122[b]	75.3[b]
Al	110.4[a]	54.5[a]	31.3[a]
	108[b]	62[b]	28.3[b]
Au	202.1[a]	174.2[a]	37.9[a]
	191[b]	162[b]	42.2[b]
Ag	161.2[a]	119.1[a]	58.1[a]
	122[b]	92[b]	45.5[b]

(b)

	C_{111}	C_{112}	C_{123}	C_{144}	C_{155}	C_{456}
Cu	−1507 [a]	−965 [a]	−71 [a]	−7 [a]	−901 [a]	45[a]
	−1271 [c]	−814 [c]	−50 [c]	−3 [c]	−780 [c]	−95 [c]
	−1500 [c]	−850 [c]	−250 [c]	−135 [c]	−645 [c]	−16 [c]
	−2000 [d]	−1220 [d]	−500 [d]	−132 [d]	−705 [d]	25[d]
	−1190 [e]	−646 [e]	219[e]	17[e]	−800 [e]	1[e]
Al	−1253 [a]	−426 [a]	153[a]	−12 [a]	−493 [a]	−21 [a]
	−1080 [f]	−315 [f]	36[f]	−23 [f]	−340 [f]	−30 [f]
	−1224 [f]	−373 [f]	25[f]	−64 [f]	−368 [f]	−27 [f]
	−1427 [g]	−408 [g]	32[g]	−85 [g]	−396 [g]	−42 [g]
Au	−2023 [a]	−1266 [a]	−263 [a]	−63 [a]	−930 [a]	54[a]
	−1730 [c]	−922 [c]	−233 [c]	−13 [c]	−648 [c]	−12 [c]
Ag	−1012 [a]	−975 [a]	162[a]	80[a]	−759 [a]	53[a]
	−843 [c]	−529 [c]	189[c]	56[c]	−637 [c]	83[c]

(c)

	C_{1111}	C_{1112}	C_{1122}	C_{1123}	C_{1144}	C_{1155}	C_{1255}	C_{1266}	C_{1456}	C_{4444}	C_{4455}
Cu	11936[a]	6834[a]	6602[a]	−98 [a]	135[a]	6628[a]	−308 [a]	5736[a]	−417 [a]	5088[a]	−191 [a]
	9587[h]	6052[h]	6623[h]	56[h]	−287 [h]	8701[h]	−390 [h]	4100[h]	−43 [h]	6527[h]	−404 [h]
	7449[i]	4233[i]	4756[i]	−262 [i]	−262 [i]	4233[i]	−262 [i]	4756[i]	−262 [i]	4756[i]	−262 [i]
	10100[j]	5050[j]	5050[j]	0[j]	0[j]	5050[j]	0[j]	5050[j]	0[j]	5050[j]	0[j]
Al	9916[a]	2656[a]	3708[a]	−1000 [a]	−578 [a]	3554[a]	−91 [a]	4309[a]	148[a]	3329[a]	127[a]
	3900[i]	2173[i]	2471[i]	−146 [i]	−146 [i]	2173[i]	−146 [i]	2471[i]	−146 [i]	2471[i]	−146 [i]
Au	17951[a]	8729[a]	9033[a]	416[a]	691[a]	7774[a]	−752 [a]	9402[a]	−170 [a]	8352[a]	15[a]
	10300[j]	5150[j]	5150[j]	0[j]	0[j]	5150[j]	0[j]	5150[j]	0[j]	5150[j]	0[j]
Ag	13694[a]	7115[a]	6652[a]	−387 [a]	−154 [a]	5295[a]	3[a]	6718[a]	−196 [a]	5416[a]	−75 [a]
	5780[i]	3495[i]	3818[i]	−172 [i]	−172 [i]	3495[i]	−172 [i]	3818[i]	−172 [i]	3818[i]	−172 [i]
	8000[j]	4000[j]	4000[j]	0[j]	0[j]	4000[j]	0[j]	4000[j]	0[j]	4000[j]	0[j]

[a]This work.
[b]Reference 23.
[c]At 290 and 300 K from Refs. 23, 37, and 38.
[d]At 4.2 K from Ref. 37.
[e]From a total-energy calculation (Ref. 38).
[f]At 300 and 298 K from Refs. 23 and 39.
[g]At 80 K from Ref. 23.
[h]Reference 38.
[i]Reference 39, assuming the validity of Eq. (20).
[j]Reference 40, assuming the validity of Eq. (21).

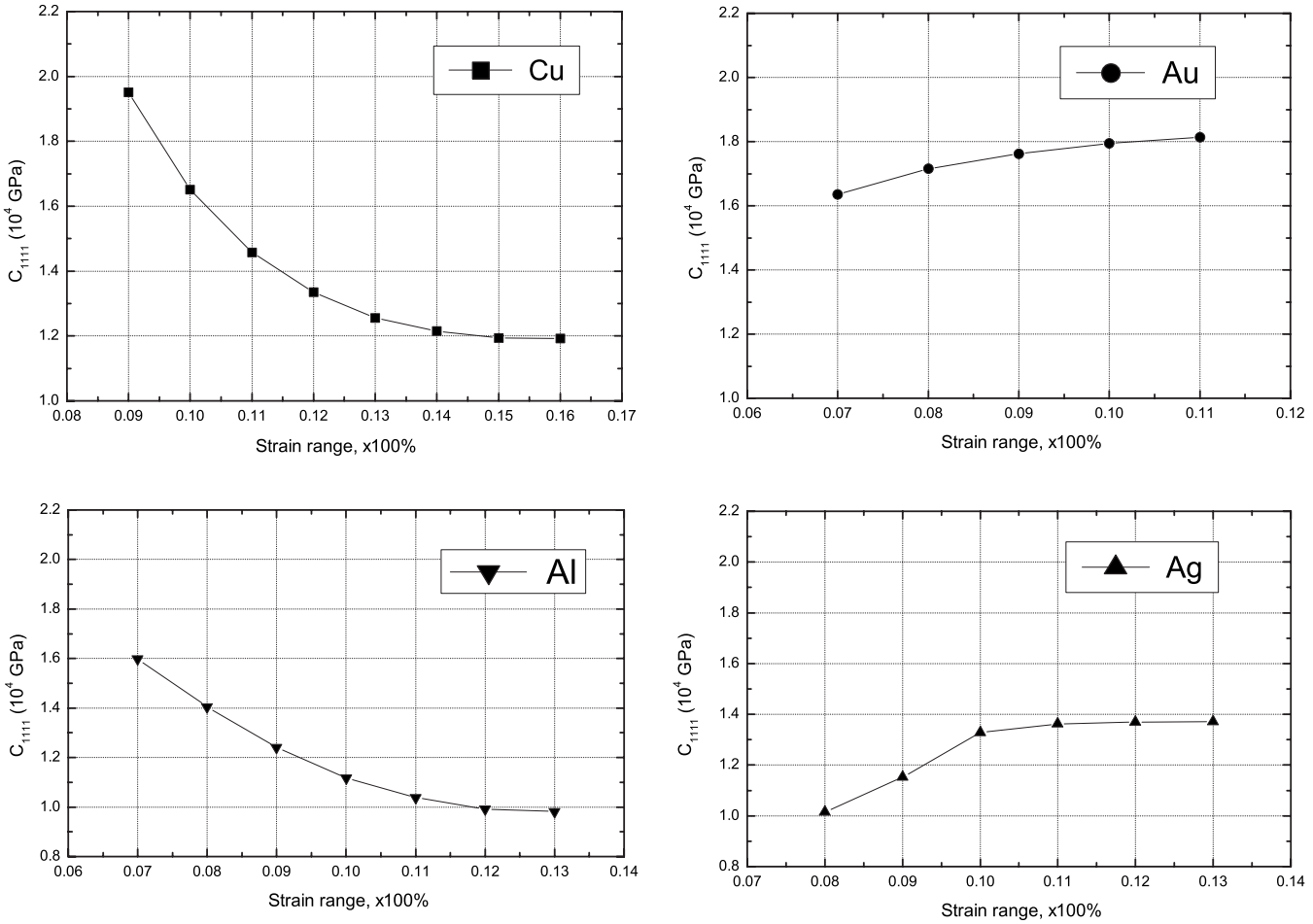

FIG. 6. (a) Cu, (b) Au, (c) Al, and (d) Ag, the fourth-order elastic constants C_{1111} vs the strain range ξ_{max}. Only at large enough strain range do those elastic constants become convergent. For Cu, Au, Al, and Ag, we selected strain ranges of 0.15, 0.10, 0.12, and 0.12, respectively.

value of ψ_4 with a larger strain. From different testing runs, we found that $\xi_{max} \sim 0.15$ is a best choice that was used in all our calculations of the internal energy function $f_A(\xi)$. With this choice, we select a series of values for ξ within $[-0.15, +0.15]$ at each strain increment $\Delta\xi = 0.0025$ and then calculate the internal energy E at a given strain ξ. The small value for $\Delta\xi$ may prolong the calculations but gives better results.

The E-ξ curves of $f_A(\xi)$ are shown in Fig. 7. The relations between E and ξ are fitted with a fourth-order polynomial and the coefficients in the polynomials are obtained numerically. Using relations in Table I, we obtain the elastic constants. The calculated FOECs are shown in (c) of Table III. Since there is no single set of FOECs known experimentally so far, the accuracy of the FOECs is difficult to judge other than just relying on the convergence test in our calculation. However, there are other theoretical estimations from the past that we can use. The values listed in (c) of Table III are from these theoretical calculations.[38–40] For this reason, we shall treat our calculation as an attempt to predict the FOECs from *ab initio* calculations. Cu is the only case where we have a complete set of FOECs from Hiki and Soma[38] who calculated all 11 independent FOECs from an approximate scheme of total energy and the homogeneous deformation method. For other fcc metals, various approximations including using empirical pair potentials and Cauchy relations were made in the calculations. As a result, the independent FOECs

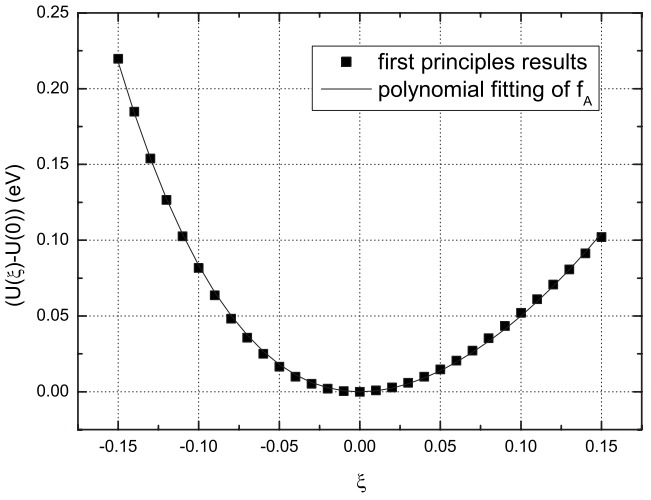

FIG. 7. The calculated change in internal energy as a function of strain for the strain tensor defined in Table I, η_A, and fitted by a fourth-order polynomial function.

are further reduced. We listed some of these results in (c) of Table III for comparison.

From the observation of the elastic constants measured from their experiment, Hiki and Granato pointed out that while the SOECs deviate from the so-called Cauchy relations much more, the TOECs follow the relations more closely,

$$C_{111} = 2C_{112} = 2C_{155},$$

$$C_{123} = C_{456} = C_{144} = 0. \quad (20)$$

In fact, our results show that indeed the SOECs are far from the Cauchy relation but the TOECs are closer. Hiki and Granato further expected that the higher-order elastic constants would follow the relations even more closely based on the argument that as the deformation strains become larger, the close-shell interactions between atoms become stronger. For Al, Rose[39] used the Cauchy relationship to estimate the FOECs,

$$C_{1112} = C_{1155},$$

$$C_{1123} = C_{1144} = C_{1255} = C_{1456} = C_{4455},$$

$$C_{1122} = C_{1266} = C_{4444}. \quad (21)$$

As a result, only four independent fourth-order elastic constants are left [see (c) of Table III]. These four independent elastic constants were then obtained using an empirical pair interaction. As for Au and Ag, Hiki *et al.*[40] utilized the generalized Cauchy relationship to obtain the following relations among some of the FOECs,

$$C_{1111} = 2C_{1112} = 2C_{1122} = 2C_{1155} = 2C_{1266} = 2C_{4444},$$

$$C_{1123} = C_{1144} = C_{1255} = C_{1456} = C_{4455} = 0, \quad (22)$$

which obviously leads to even more reduction in the number of FOECs.

Our results for both the TOECs and FOECs show that, indeed, the Cauchy relations are followed, more for FOECs than TOECs, given the possible errors in our calculations. For example, for the FOECs for Cu, we have $C_{1111}/C_{1112} = 1.75$, which is very close to the ratios for C_{1111}/C_{1122} and C_{1111}/C_{1155}. And C_{1111}/C_{1266} and C_{1111}/C_{4444} are close to 2.0. The values of C_{1123}, C_{1144}, C_{1255}, C_{1456}, and C_{4455} are very small as compared with the rest of the FOECs. The same trend can be found for the rest of fcc metals.

V. CONCLUSIONS

In this work, we represented a systematic scheme to compute the second- and high-order elastic constants for four fcc metals using the DFT and homogeneous deformation method. In principle, this scheme can apply to single crystalline systems with arbitrary symmetry. Our theoretical results are in excellent agreement with experimental results for the SOECs which are available from many measurements. For the TOECs, the agreement with the available experimental data is very well also considering the sparsity of the experimental data and also the errors resulting from the difficulties in the measurements. Built on the results from the SOECs and TOECs, we took a step forward to calculate the FOECs. While the experimental data are still not available for those metals, our results are quite well inline with the trends predicted from other theoretical calculations and estimates. Our results in the higher-order elastic constants provide support for Hiki and Granato's expectation that as the atomic repulsion becomes stronger at large deformation strain, the higher-order elastic constants would follow more closely the Cauchy relations. Since there are fewer experimental data available for TOECs and none for FOECs even to date, our results of the FOECs are predicted values which may serve as a valuable guide or reference for experimenters which would someday perform a measurement. On the other hand, we are quite encouraged by the overall results as a proof of the applicability of the DFT calculation for such highly sensitive quantities as the TOECs and the FOECs.

ACKNOWLEDGMENTS

The authors are grateful for the financial support of this work provided by the U.S. Army Research Office (USARO) under Contract No. ARO-W911NF-07-1-0490 and DARPA SAM II through ONR under Contract No. N00014-06-1-0490.

*Corresponding author; mo.li@mse.gatech

[1] M. Born and K. Huang, *Dynamical Theory of Crystal Lattices* (Oxford University Press, London, 1956).
[2] D. C. Wallace, *Thermodynamics of Crystals* (Dover, New York, 1998).
[3] F. Birch, Phys. Rev. **71**, 809 (1947).
[4] F. Murnaghan, *Finite Deformation of an Elastic Solid* (Wiley, New York, 1951).
[5] S. Bhagavantam, *Crystal Symmetry and Physical Properties* (Academic, New York, 1966).
[6] R. Thurston and K. Brugger, Phys. Rev. **133**, A1604 (1964).
[7] K. Brugger, Phys. Rev. **133**, A1611 (1964).
[8] P. B. Ghate, J. Appl. Phys. **35**, 337 (1964).
[9] J. M. Ziman, *Electrons and Phonons* (Clarendon, Oxford, 1960).
[10] B. P. Barua and S. K. Sinha, J. Appl. Phys. **49**, 3967 (1978).
[11] S. Chantasiriwan and F. Milstein, Phys. Rev. B **58**, 5996 (1998).
[12] R. Kato and J. Hama, J. Phys.: Condens. Matter **6**, 7617 (1994).
[13] S. P. Lepkowski and J. A. Majewski, Solid State Commun. **131**, 763 (2004).
[14] S. P. Lepkowski, J. A. Majewski, and G. Jurczak, Phys. Rev. B **72**, 245201 (2005).
[15] K. Shimada, T. Sota, K. Suzuki, and H. Okumura, Jpn. J. Appl. Phys., Part 2 **37**, L1421 (1998).
[16] G. Bester, X. Wu, D. Vanderbilt, and A. Zunger, Phys. Rev. Lett. **96**, 187602 (2006).
[17] H. F. Tiersten, J. Acoust. Soc. Am. **57**, 667 (1975).

[18] J. S. Yang, Acta Mech. **196**, 103 (2008).
[19] R. N. Thurston and M. J. Shapiro, J. Acoust. Soc. Am. **41**, 1112 (1967).
[20] R. Fowles, J. Geophys. Res. **72**, 5729 (1967).
[21] R. A. Graham, Phys. Rev. B **6**, 4779 (1972).
[22] A. N. Abd-alla, Mech. Res. Commun. **26**, 335 (1999).
[23] *Second and Higher Order Elastic Constants*, Landolt-Börnstein, New Series, Group III, Vol. 29A, edited by A. G. Every and A. K. McCurdy (Springer-Verlag, Berlin, 1992).
[24] P. N. Keating, Phys. Rev. **145**, 637 (1966).
[25] P. N. Keating, Phys. Rev. **149**, 674 (1966).
[26] T. Çağin and J. R. Ray, Phys. Rev. B **38**, 7940 (1988).
[27] T. Çağin and B. M. Pettitt, Phys. Rev. B **39**, 12484 (1989).
[28] R. Srinivasan, Phys. Rev. **144**, 620 (1966).
[29] O. H. Nielsen and R. M. Martin, Phys. Rev. B **32**, 3792 (1985).
[30] O. H. Nielsen, Phys. Rev. B **34**, 5808 (1986).
[31] J. Sörgel and U. Scherz, Eur. Phys. J. B **5**, 45 (1998).
[32] J. Zhao, J. M. Winey, and Y. M. Gupta, Phys. Rev. B **75**, 094105 (2007).
[33] M. Lopuszynski and J. A. Majewski, Phys. Rev. B **76**, 045202 (2007).
[34] G. Kresse and J. Furthmuller, Phys. Rev. B **54**, 11169 (1996).
[35] D. Vanderbilt, Phys. Rev. B **41**, 7892 (1990).
[36] *American Institute of Physics Handbook*, 3rd ed. (McGraw-Hill, New York, 1970).
[37] K. Salama and G. A. Alers, Phys. Rev. **161**, 673 (1967).
[38] H. Soma and Y. Hiki, J. Phys. Soc. Jpn. **37**, 544 (1974).
[39] M. F. Rose, Phys. Status Solidi **17**, K199 (1966).
[40] Y. Hiki, J. R. Thomas, and A. V. Granato, Phys. Rev. **153**, 764 (1967).
[41] C. Bercegeay and S. Bernard, Phys. Rev. B **72**, 214101 (2005).
[42] Y. Hiki and A. V. Granato, Phys. Rev. **144**, 411 (1966).